Design of a Fully-Soft Lift-Assist Wearable Suit Powered by Flat Inflatable Artificial Muscles

Taehwa Hong, Chihyeong Lee, Shinwon Chang, Eunsik Choi, Beomdo Kim, Jooeun Ahn, and Yong-Lae Park, *Member, IEEE*

***Abstract*—The development of soft pneumatic actuators has expanded their applications due to flexibility and adaptability in wearable systems. Among these, flat inflatable artificial muscles (FIAMs) show a significant potential for wearable robots designed to assist body movements. While existing devices focus on supporting specific joints, an integrated system for multiple joints has not yet been realized. This study introduces a fully soft wearable suit incorporating FIAMs to assist lifting motions through combined actuation of the arms and back. The design and fabrication process of FIAMs are described, along with a force estimation model adapted for integration with the wearable suit. The experimental validation demonstrates robust and consistent performance of FIAMs under cyclic testing. The modular structure allows seamless integration into the wearable suit, enabling active assistance for targeted muscle groups. Human testing is conducted using weight-lifting tasks to evaluate the suit. Muscle activation and respiratory indices are measured to quantify the effects of the suit. The results demonstrate a partial reduction in metabolic cost expenditure, indicating the potential of this wearable suit for physical assistance in daily and occupational tasks.**

***Index Terms*—Soft robotics, wearable robotics, soft exosuit, lift assistance, pneumatic artificial muscles.**

Fig. 1. Integrated assistive suit equipped with FIAMs. Two parallel artificial muscles are connected to the back, and another two are connected to the upper arm, respectively. This suit is designed to support general lifting motions, primarily utilizing the muscles of the back and upper arms.

I. Introduction

THE field of assistive wearable devices has witnessed significant advancements, especially with the integration of various actuators [1], [2], [3], [4]. A notable development in this domain is the incorporation of soft actuators, which have played a key role in the evolution of assistive devices [5], [6], [7], [8]. The safe actuation and structural compliance make soft actuators particularly beneficial in scenarios involved with human interactions [9], [10], [11]. This is crucial for devices aimed at supporting labor-intensive tasks, such as lifting heavy loads, where safety and adaptability are key considerations [4], [12].

Pneumatic artificial muscles (PAMs), a specific type of soft actuators, have become a promising solution for wearable devices designed to reduce the need for human labor [13]. The ability to generate forces comparable to human muscles, along with their inherent flexibility, makes PAMs an ideal choice for such applications [14], [15]. The development of assistive suits using compliant actuation mechanisms, including soft pneumatic actuators [16], [17] and electro-pneumatic pumps [18], has shown a potential in helping workers perform tasks more efficiently and with a reduced risk of injury.

Among different types of soft pneumatic actuators, this study focuses on flat inflatable artificial muscles (FIAM) [8], [19], also known as pouch motor actuators [20]. The unique attributes of these actuators make them an excellent choice for actively supportive and assistive wearable devices. FIAMs are extremely lightweight, consisting of a stack of multiple fabric sheets. The components that supply pressurized air are also light enough to be portable and easily integrated into the host systems, i.e., wearable suits. In addition, they remain compact, whether inflated or not, ensuring that the wearer's workspace is not disturbed. Furthermore, as no rigid components are required

Received 15 August 2024; accepted 1 February 2025. Date of publication 13 February 2025; date of current version 26 March 2025. This article was recommended for publication by Associate Editor K.-U. Kyung and Editor C. Laschi upon evaluation of the reviewers' comments. This work was supported in part by the National Research Foundation under Grant RS-2023-00208052 and in part by the Technology Innovation Program under Grant 20008912, funded by the Korea Government (MSIT and MOTIE, respectively). *(Taehwa Hong, Chihyeong Lee, and Shinwon Chang contributed equally to this work.) (Corresponding authors: Jooeun Ahn; Yong-Lae Park.)*

This work involved human subjects or animals in its research. Approval of all ethical and experimental procedures and protocols was granted by Institutional Review Board of Seoul National University under Application No. IRB No. 2112/002-008, and performed in line with the Helsinki Declaration.

Taehwa Hong, Shinwon Chang, and Yong-Lae Park are with the Soft Robotics and Bionics Laboratory in the Department of Mechanical Engineering; Institute of Advanced Machines and Design; Institute of Engineering Research, Seoul National University, Seoul 08826, South Korea (e-mail: ndolphin93@snu.ac.kr; austin323@snu.ac.kr; ylpark@snu.ac.kr).

Chihyeong Lee, Eunsik Choi, Beomdo Kim, and Jooeun Ahn are with the Sports Engineering Laboratory in the Department of Physical Education; Institute of Sport Science, Seoul National University, Seoul 08826, South Korea (e-mail: chi0412@snu.ac.kr; ces4032@snu.ac.kr; kimbd0819@snu.ac.kr; ahnjooeun@snu.ac.kr).

This article has supplementary downloadable material available at https://doi.org/10.1109/LRA.2025.3541377, provided by the authors.

Digital Object Identifier 10.1109/LRA.2025.3541377

in general, FIAMs hardly have the risk of potentially harming the wearer. Most importantly, they are capable of generating substantial contraction force, making them a reliable option for mechanisms for assistive or wearable devices.

Despite the efforts on improving the actuation performance [19], [21], [22], challenges remain when integrating them into a fully-soft wearable suit for simultaneous multi-joint assistance. One major issue is the efficient positioning of the actuator to support the desired muscle group without using rigid frames commonly found in conventional exoskeletons, leading to a compromise between comfort and performance. The anchoring method thus becomes crucial to effectively transmit desired forces or torques to the target regions. However, an emphasis on effective anchoring can result in a device that is both heavy and uncomfortable, posing a challenge for user wearability. Enhancements in the anchoring suit could be realized by balancing the wearability with the actuator performance. Another notable limitation of pneumatic actuators is the need for heavy components to supply compressed air. Even though the actuator itself may be lightweight and compact, the cumbersome supply system often compromises portability and makes it difficult to integrate actuators into wearable suits in an untethered manner. Furthermore, wearable suits employing soft actuators sometimes lack quantitative methods for evaluating their effectiveness. Beyond assessing the actuator performance, muscle activation and metabolic analyses are essential to providing a quantitative index that measures the effect of wearing the system.

Addressing these challenges, we propose an assistive suit that integrates FIAMs with a lightweight anchoring suit to actively support lifting tasks. The modular design of the artificial muscles allows for easy customization of the anchoring suits for various tasks. We also developed a compact and lightweight air supply system to maintain the desired force and contraction ratio of the artificial muscles untethered. The anchoring suit, designed with wearability and performance in consideration, can be equipped with multiple artificial muscles. Our study extends to measuring the electrical signals of the wearer's muscles and the respiratory data during tasks to propose indices for interpreting and estimating muscle usage and energy expenditure. These indices aim to provide a quantitative assessment of the performance of the system, offering a comprehensive understanding of its effectiveness.

II. Materials and Methods

A. Wearable Suit Design

1) Anchoring Harness: The suit was designed to assist lifting motions, focusing on supporting the arm and back muscles. It comprises two main components: the anchoring frame and multiple FIAMs. Based on a prior design [23], the harness-like anchoring mechanism uses straps and elastic bands to secure key skeletal regions, providing fixed points to counteract forces generated by the artificial muscles (Fig. 2). Anchoring regions include knee bands covering the femur and tibia, a central waistband, and straps for the shoulders and forearms. Two parallel straps running from the shoulders to the knees distribute the load across the body. The design prioritizes minimizing weight while maintaining functionality for lifting tasks. Non-stretchable nylon webbing effectively transmits forces, while high-stiffness rubber bands are used sparingly to avoid restricting natural movement. The stiffness of these components, as well as their compliance, was carefully validated to ensure both effective force transmission and wearer comfort based on prior user studies [23].

2) Flat Inflatable Artificial Muscles: With the structure of the suit established, the actuation part of the system was designed. The FIAMs were fabricated using heat-sealing and laser cutting, as shown in Fig. 3(a). They were made of two nylon fiber sheets coated with thermoplastic polyurethane (TPU) (N210D, U-LongTech) on both sides, with a thickness of 0.2 mm. The TPU-coated nylon sheet was selected for its high tensile strength, durability, flexibility, airtightness, and compatibility with ultrasonic welding, making it ideal for sustaining repeated actuation cycles [19], [24]. This combination ensures a balance between durability and compliance, critical for a reliable actuation performance. The thickness of 0.2 mm was determined as a trade-off. While thinner material makes actuators more responsive but less durable, thicker material provides greater strength but slower actuation.

The heat-sealing process was conducted using a custom-designed ultrasonic welding device with a 3 mm round-shaped tooltip mounted on a motorized $x - y - z$ stage, as shown in Figs. 3(b). The predefined welding pattern ensured uniform and robust seams for the FIAMs. To enhance contraction force and achieve a higher contraction ratio, two FIAMs were joined through additional welding, as shown in Fig. 3(c).

The dimensions of the artificial muscles, 100 mm in width (D) and 400 mm in length (L_0), were selected to provide sufficient coverage for the arm and back regions, scaled to match the participants' body for effective assistance. After fabrication by ultrasonic welding, the artificial muscles were laser-cut to remove excess material, as shown in Fig. 3(a). The welding pattern is composed of rectangles with chamfered corners connected serially. The chamfered corners reduce the undesired wrinkles that emerge along the sides of the inflatable muscle. Hence, the FIAM in an inflated state resembles a union of cylindrical shapes as described in the following section. The cylindrical shape of the muscles facilitated smooth contraction and minimal stress concentrations, ensuring even actuation during operation. These material and design choices align with those used in similar soft actuator developments, where TPU-coated nylon sheets are valued for their versatility and durability [24].

3) Integration of Artificial Muscles: Four artificial muscles, comprising two for the arms and two for the back, were integrated into the anchoring harness. Each arm muscle was affixed to the anterior part of the upper arm, while the back muscles were placed posteriorly near the hip to mitigate the lateral movement of the hip during back extensions, as shown in Fig 2(a). Buckles at both ends of the artificial muscles allowed for their easy installation and replacement on the suit.

To make the assistive suit untethered, a control board, solenoid valves, and a power source were designed to be integrated within the central belt. A portable miniature pump (B2C-090V12AN-03, Parker) was selected for the actuation of each artificial muscle and able to provide a pressure of up to 20 kPa with a flow rate of 9.5 L/min. To manage airflow the direction with only a single pump, two 3-way solenoid valves (VK332 V, SMC) were employed. The binary control of the solenoid valves alternates between inflating and deflating the artificial muscles, enabling directional control of the airflow. Unlike systems that passively release air back to the ambient atmospheric pressure, this design actively redirects airflow, ensuring controlled deflation and

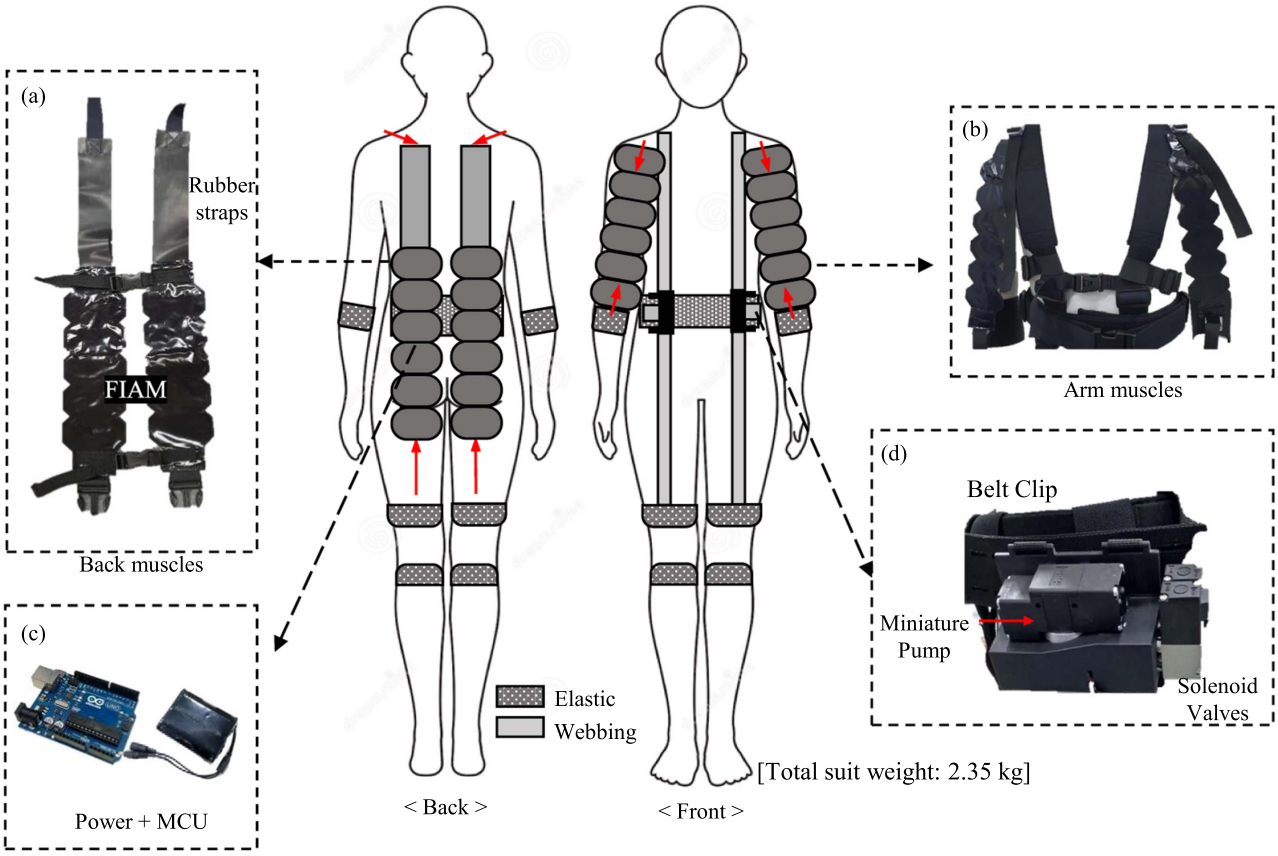

Fig. 2. The central figure illustrates the back and the front views of the suit when worn by the users. (a) Parallel artificial muscles were connected using non-stretchable bands, designed as modular units for easy attachment or detachment from the anchoring suit. (b) Two artificial muscles extend from the shoulder to the lower arm, with the actuators precisely aligned with the upper arm muscles' contraction direction for efficient support. (c) Batteries and controller board are attached to the central belt, making the system untethered. (d) The rechargeable battery pack and the miniature pump, along with the solenoid valves, are compactly integrated onto the designed manifold and secured to the belt.

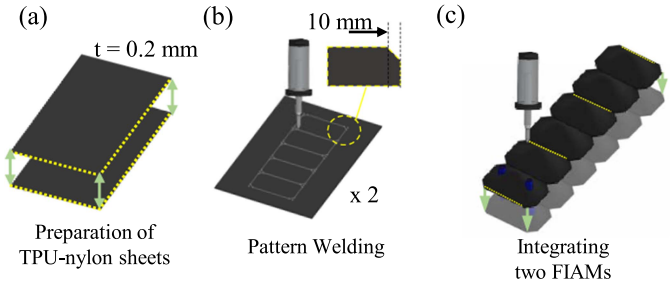

Fig. 3. Fabrication process of a FIAM. (a) Two TPU-coated nylon sheets of the identical size are aligned together. (b) A predesigned sketch of the artificial muscle, with chamfered corners is patterned by ultrasonic welding for bonding of the patterned trajectory. (c) Two identical FIAMs are aligned and fused by welding additional horizontal lines.

precise adjustment of the contraction and relaxation phases of the artificial muscles, as shown in Fig. 2(d).

The integration of these components into the central belt provides the benefits of portability, comfort, and usability, making the system suitable for wearable applications. Unlike conventional systems that often require external air supply or bulky components [18], [20], this compact configuration allows the suit to operate untethered while maintaining high performance and reliability. Additionally, the modular design of the air supply system simplifies the assembly and enables easy adaptation to different wearable setups [16], [17].

A micro-controller board (UNO, Arduino) was incorporated to control the pressure of the pump and the direction of the airflow through the valves. A 12V-6400 mAh capacity rechargeable lithium-ion battery was connected alongside the microcontroller board to the circuit, ensuring the operation of the actuators and control components, as shown in Fig. 2(c). This placement not only maximized the functionality but also allowed the wearer's freedom of movement, making the entire system self-contained and efficient for practical use.

B. Characterization of Flat Inflatable Artificial Muscles

1) Axial Contraction: The axial contraction behavior of the artificial muscles aligns with previously established models [19], [22]. The relationship between axial force (F_a) and internal pressure is expressed using virtual work principles as:

$$-F_a dL = PdV, \tag{1}$$

where L is the actuator's contracting length, and V is the pouch volume [25]. The axial force can be parameterized by θ as:

$$F_a(\theta) = -P\frac{dV}{dL} = L_0 D P \frac{\cos\theta}{\theta}, \tag{2}$$

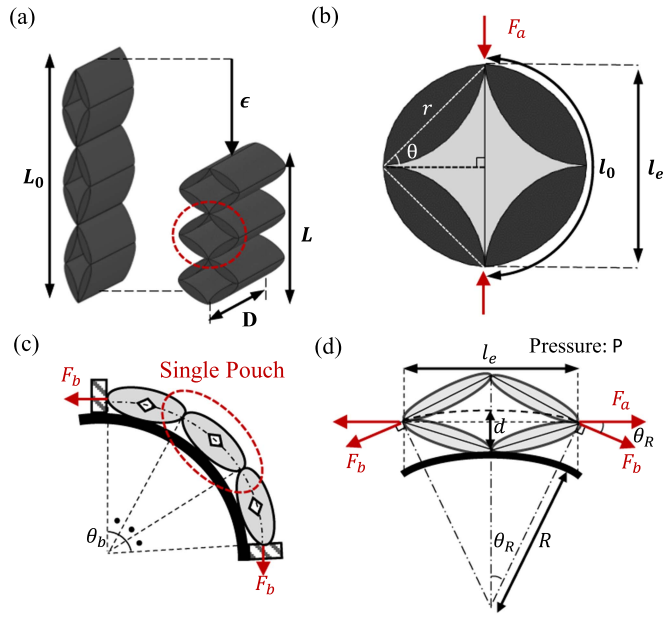

Fig. 4. (a) The FIAM configuration during the pressurization and the predefined parameters. (b) Detailed illustration of a single pouch, showing geometric parameters. (c) The bending actuation of the FIAM on a curved surface. (d) External forces and geometric parameters affecting a single pouch under bending.

with strain ϵ defined as:

$$\epsilon = \frac{l_0 - l_e}{l_e} \cong 1 - \frac{\sin \alpha\theta}{\alpha\theta}. \tag{3}$$

Using prior models [21], [22], a fitting coefficient $\alpha = 1.1$ was applied for alignment with experimental data. The estimated force $\hat{F}_a$ is defined as a function of strain and pressure:

$$\hat{F}_a = \mathcal{F}(\epsilon, P). \tag{4}$$

Numerical solutions for $\hat{F}_a$ were obtained using (2) and (3).

2) Contraction While Bending: The bending behavior of artificial muscles on curved surfaces was analyzed to derive the relationship between the bending angle (θ_b) and the contraction force (F_b). Assuming constant curvature and identical deformation across three connected pouches, the effective bending angle per pouch (θ_R) is:

$$\theta_R = \frac{\theta_b}{2N}, \tag{5}$$

where N is the number of pouches. The effective length (l_e) in bending is calculated as:

$$l_e = 2(R + d)\sin\theta_R, \tag{6}$$

where R is the radius of curvature and d is the offset. Using (3), the strain allows estimation of horizontal force (F_a). The contraction force (F_b) is then defined as:

$$\hat{F}_b = F_a \cos\theta_R = \mathcal{F}(\epsilon_b, P)\cos\theta_R. \tag{7}$$

Experimental data confirmed the validity of (4) and (7), as detailed in Section IV.

C. Surface Electromyography (sEMG) Measurement

To evaluate the developed system objectively, we monitored the muscle activation level and energy expenditure. By tracking muscle activation, we aimed to quantify the extent of support the suit provided to the wearer during the designed tasks. The integration of the voltage levels measured from surface electromyography (sEMG) on targeted muscles, known as the integrated EMG value (*iEMG*), served as the primary method for evaluating muscle activation [26], [27]. The electromyography (EMG) and the energy expenditure (EE) measurements were employed to evaluate the system's effectiveness in reducing the muscle activation level and the metabolic cost during weight-lifting tasks. Since these are standard evaluation techniques [28], [29], their combined application in the context of a fully soft assistive suit incorporating FIAMs introduces a novel framework for performance assessment. This approach allows for a detailed understanding of the system's impact on muscle usage and energy efficiency, supporting the feasibility of pneumatic actuators for wearable applications.

The voltage from the target muscle was integrated over a specified time window [t, t+T], represented by the equation

$$iEMG = \int_t^{t+T} |V_{EMG}(t)|\, dt, \tag{8}$$

where $V_{EMG}(t)$ was the voltage measured at time t. For inter-participant comparison, the *iEMG* value was normalized as

$$iEMG_N = \frac{iEMG}{RVC}\,[\%], \tag{9}$$

with the reference voluntary contraction (RVC) representing the peak voltage value of the EMG signal within all the measurements. Prior to task initiation, each participant was fitted with EMG measurement devices. The primary muscles monitored are the erector spinae (ES), gluteus maximus (GM), and biceps femoris (BF), which were predominantly engaged during weight-lifting activities.

D. Energy Expenditure

In conjunction with the muscle activation, a respiratory-related index was measured. During the task implements the oxygen volume inhaled per minute and weight (VO_2) and the carbon dioxide volume exhaled per minute and weight (VCO_2) of each participant were measured. Referring to the prior studies that estimated the energy expenditure per minute (EEm) using VO_2 and VCO_2 levels [30], [31], [32], calculated as a weighted sum of these values, such as

$$EEm = 16.89\, VO_2 + 4.84\, VCO_2 \tag{10}$$

III. Experiments

A. Actuator Characterization

To evaluate the axial actuation of the artificial muscles, two sets of experiments were performed: one focusing on linear contraction and the other on bending.

1) Linear Actuation of FIAMs: A tensile tester (34sc-1, Instron) measured the contraction force of the muscle generated at various pressure levels, ranging from 10 kPa to 50 kPa with an increment of 10 kPa. The force and contraction ratios were then recorded under quasi-static conditions at a displacement speed

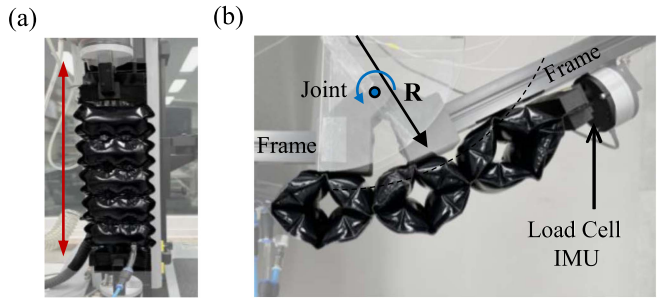

Fig. 5. (a) Experimental setup for characterizing the linear contraction of the artificial muscle. The artificial muscle was pressurized at a constant pressure, and the force generated was measured while the tensile tester head moved at a fixed speed. (b) Experimental setup for the bending actuation of the artificial muscle on a curved surface. The artificial muscle was anchored to a frame with a rotational joint, with one end connected to a load cell.

of 0.1 mm/s, with a cyclic of 20 times at each pressure level, as depicted in Fig. 5(a).

2) Bending Actuation of FIAMs: This experiment simulated human bending motions using a single-joint aluminum linkage. One end of the muscle was fixed to one link, and the other end was attached to a load cell (RFT64-6A01, Robotus) anchored to the second link. The load cell measured force during bending, while an IMU (EBIMU-9DOF, E2BOX) recorded the bending angle (θ_b), synchronized with the force data (Fig. 5(b)).

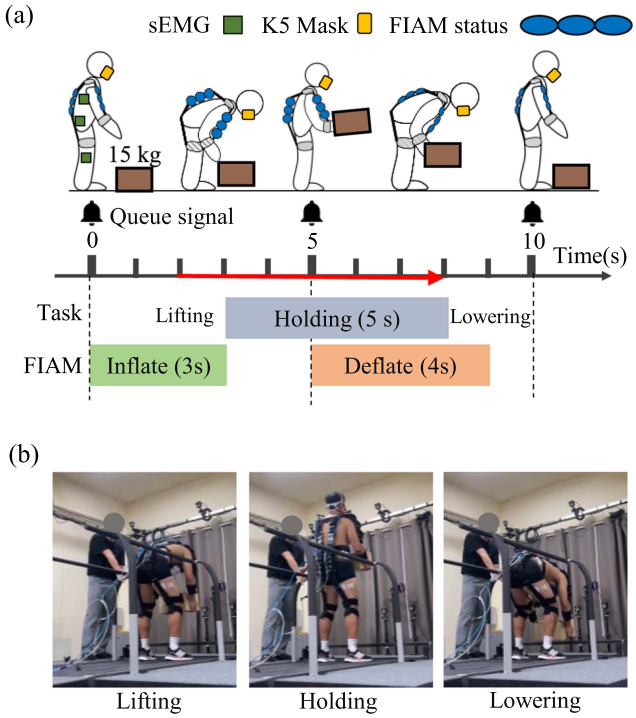

Fig. 6. (a) Illustration of the timing schedule for the lifting task, showing the sequence of lifting, holding, and lowering a 15 kg load over 10 seconds alongside the corresponding artificial muscle actuation. (b) A participant wearing the assistive suit performs the lifting task, equipped with EMG devices and a respiratory mask.

B. Clinical Test

1) Lifting Task Protocol: The clinical evaluation aimed to assess the performance of the wearable suit with FIAMs during a weight lifting task. Each participant lifted a 15 kg weight, performing the task in three distinct phases: lifting, holding, and lowering. Each phase lasted for 10 seconds, creating a controlled cycle of 30 repetitions to ensure consistent and repeatable conditions across all trials. Participants were not provided with specific posture instructions to allow for natural movement patterns, reflecting realistic lifting scenarios.

The weight selection of 15 kg was based on research conducted in the United States, which highlights that approximately 30% of occupational injuries are caused by manual handling tasks involving weights around 23 kg [33]. This choice balances the need for a meaningful load with the constraints imposed by the device's power output and safety considerations. Additionally, the Institutional Review Board (IRB) required adherence to safety guidelines to protect participants during human trials. Allowing participants to lift significantly more than 15 kg would not comply with these standards.

The participant group included five males aged between 20 and 30, representing a typical adult population with moderate physical fitness. Each participant performed the task under three conditions: lifting without wearing the suit (None), wearing the suit but without actuation (Off), and wearing the suit with the actuators fully engaged (On). The sequence of trials for the three conditions was randomized for each participant to minimize the influence of fatigue or adaptation on the results. This procedure provided a robust dataset for analyzing the effect of the wearable suit and actuation on lifting performance, muscle engagement, and respiratory indices.

2) Actuator Control Scheme: The back and arm FIAMs were actuated in a synchronized manner, providing assistance during the lifting motion and targeting specific muscle groups engaged in the task. The actuation strategy, illustrated in Fig. 6(a), ensured alignment with the participants' natural lifting and lowering movements. Inflation of the FIAMs required approximately three seconds, a duration selected to match the actuator response time and maintain stable force output. Deflation was completed within four seconds, allowing a smooth transition during the lowering motion while avoiding abrupt changes in support.

The timing of FIAM activation was carefully synchronized with the lifting and lowering phases of the participants' movements. Activation of the actuators was completed before the "Lifting" signal, ensuring that full support was available as the lifting began. This pre-activation phase ensured alignment of the actuator's force output with the initial effort required for the task. Deflation timing was similarly adjusted to align with the lowering phase, maintaining consistent assistance while minimizing resistance. The structure of each lifting task followed a five-second cycle, accommodating the inflation and deflation phases and providing reliable assistance throughout the experiment.

3) Measurement Devices: To assess muscle activation and metabolic cost as described in Sections II-C and II-D, two measurement devices were used. The sEMG devices (Trigno Mini, Delsys) were affixed to the target muscles based on established placement protocols [34]. These devices measured the electrical activity of the muscles during the lifting tasks, providing data on muscle engagement across different experimental conditions.

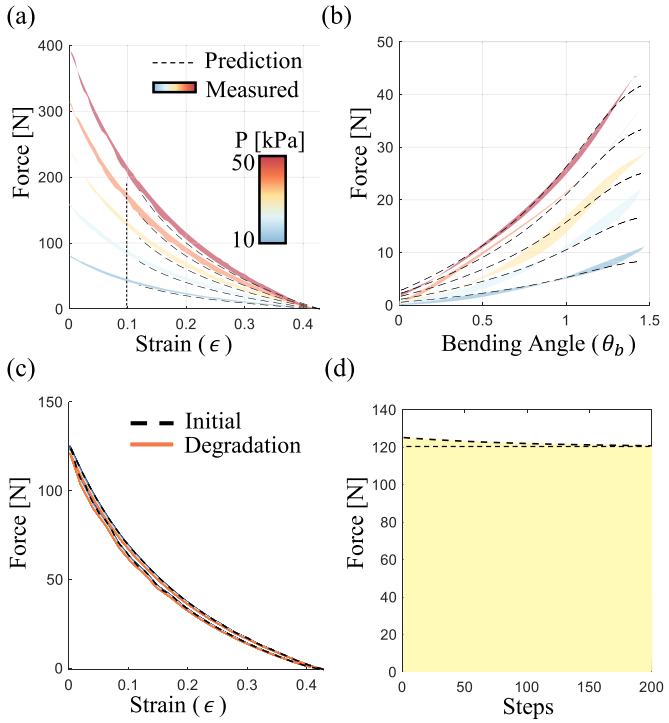

Fig. 7. (a) Axial force vs. strain curves for the FIAM measured under five different pressure inputs, with dashed lines representing prediction curves. (b) Force measurements of the FIAM under bending deformation using the same pressure inputs as in the axial deformation tests. (c) Axial force vs. strain curves recorded during cyclic testing. (d) Maximum peak force degradation observed throughout the cyclic testing.

Metabolic cost was evaluated using a respiratory gas analysis system (K5, COSMED). The system recorded oxygen consumption (VO_2) and carbon dioxide production (VCO_2) wirelessly during the task. The collected data were used to calculate the energy expenditure per minute (EEm) based on (10), which accounts for the respiratory exchange ratio (RER). The mask was securely fitted to each participant to ensure accurate and continuous monitoring of respiratory gases throughout the lifting cycles, as shown in Fig. 6(a).

IV. Results

A. FIAM Performance

The characterization results for both axial and bending experiments are presented in Fig. 7(a) and (b), respectively, demonstrating the performance and predictive accuracy of the developed model under different actuation scenarios.

For the axial contraction tests, the experimental results showed strong alignment with the model predictions derived from (3). Across the tested strain range of 0.1 to 0.43, the forces generated at all applied pressure levels matched closely with the theoretical estimates. The shaded regions in Fig. 7(a) indicate the range of experimental variability, with an average force deviation of 4.24 N between the experimental and model-predicted values. The corresponding estimation error was calculated to be 8.72 N on average, demonstrating a reliable force-strain relationship. These results confirm the model's ability to accurately capture the behavior of the actuator under axial loads, ensuring consistency in practical applications.

The cyclic performance of the artificial muscles was further evaluated under an actuation pressure of 50 kPa, focusing on short-term reliability and repeatability. Fig. 7(c) and (d) illustrate the cyclic axial force-strain behavior over 200 cycles. The maximum force degradation was observed to be minimal, with a reduction of only 1.52% between the initial and final cycles, as shown in Fig. 7(c). The nearly overlapping force-strain curves across the cycles indicate consistent performance, confirming the actuator's structural integrity and resistance to material fatigue. Fig. 7(d) highlights the gradual reduction in peak force, which suggests negligible wear and ensures reliable operation over short-term repetitive cycles. These findings validate the actuator's durability under repeated use.

For the bending actuators, the experimental forces generated during actuation closely matched the model predictions across varying bending angles (θ_b) and pressure levels, confirming the applicability of the force estimation model under geometric constraints. The experimentally measured bending angles were applied to (7), which predicted the forces with high accuracy. As shown in Fig. 7(b), the average deviation between the measured and predicted forces was 2.31 N, while the estimation error averaged 1.73 N. These results indicate that the bending force model successfully estimates the nonlinearities occured by the complex geometry and the material deformation of the FIAM during the bending, further demonstrating its robustness for practical implementation.

Overall, the axial and bending characterization results establish the validity of the proposed models for force estimation, their consistency across different loading conditions, and the reliability of the FIAM during repetitive cycles.

B. Muscle Activation and Metabolic Cost Analysis

The analysis evaluated the impact of the assistive suit on muscle activation and energy consumption during the lifting tasks. The normalized $iEMG_N$ values were calculated for all participants, focusing on reduction ratios across three conditions (None, Off, and On) of the suit and two separated phases (lifting and lowering) of the task. Whereas *EEm* was calculated for the entire task operation. Two key ratio indices were derived:

- <None-On>: represents the overall support from wearing the suit and activating the artificial muscles.
- <Off-On>: reflects the effect of the active artificial muscle support, excluding the passive benefits from wearing the suit.

Table I presents the experimental results for all five participants, comparing $iEMG_N$ and *EEm* across the three conditions (None, Off, and On). Missing data points are marked as "-", indicating failed measurements of $iEMG_N$ from the BF muscle due to the EMG device interference caused by the suit.

Reduction ratios for $iEMG_N$ and *EEm* across three target muscles, three conditions, and two phases are summarized in Table I. The values highlighted in green indicate decreases in both indices for the <None-On> case. Notable reductions in muscle activation were observed for participants 1, 3, and 4, with significant decreases in GM and BF muscles for participants 3 and 4.

No significant differences were observed between the two phases of the motion. Participants who exhibited reductions in muscle activation tended to benefit during both the lifting and the lowering phases. In contrast, participants such as 2 and 5 did not show a noticeable effect from the suit's assistance.

TABLE I
CLINICAL TEST RESULTS FOR FIVE PARTICIPANTS

			Participant 1			Participant 2			Participant 3			Participant 4			Participant 5		
			None	Off	On	None	Off	On	None	Off	On	None	Off	On	None	Off	On
$iEMG_N$ [%]	Lifting	ES	65.76	**74.96**	**65.58**	47.75	**63.10**	**60.33**	78.05	**57.64**	**53.26**	52.85	**83.27**	**83.09**	21.66	21.98	45.49
		GM	74.17	**87.81**	**75.89**	20.33	21.13	28.98	25.82	14.47	15.22	24.02	**91.08**	**87.40**	22.24	28.81	46.75
		BF	26.63	50.31	53.36	-	-	-	39.97	**38.99**	**37.87**	39.52	**17.74**	**8.93**	-	-	-
	Lowering	ES	42.37	**42.76**	**37.44**	25.81	36.01	42.98	65.77	**49.93**	**48.28**	66.70	57.46	**57.47**	19.16	18.34	50.21
		GM	57.37	42.76	58.99	8.63	10.43	13.75	15.52	**5.46**	**5.28**	20.20	50.55	51.93	11.14	14.44	32.85
		BF	23.24	**41.31**	**39.46**	-	-	-	61.98	64.64	76.59	57.66	**76.95**	**42.96**	-	-	-
EEm [kcal/min ·kg]			8.227	7.340	**8.212**	6.093	6.009	6.346	7.751	**8.566**	**8.290**	5.541	**5.947**	**5.558**	7.690	**8.002**	**6.824**

<None-On> case reduction <Off-On> case reduction

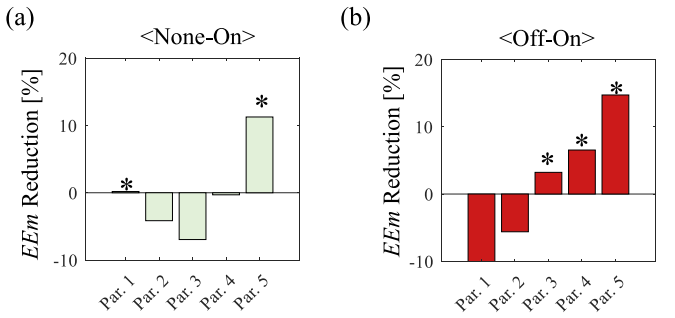

Fig. 8. Decrease in *EEm* of the participants. Two comparison cases are plotted: "None vs. On" in (a) and "Off vs. On" in (b). The "*" mark indicates the participants who exhibited a reduction in metabolic cost.

For the <Off-On> case, reductions in $iEMG_N$ were more commonly observed, as highlighted with red dashed boxes in Table I. For participants 1, 3, and 4, most muscles showed reductions in both phases. Reductions in *EEm* were observed for participants 3 (3.22%), 4 (6.54%), and 5 (14.72%), as shown in Fig. 8(b).

V. DISCUSSION

This work introduced a fully soft assistive suit integrated with FIAMs, specifically designed for weight-lifting tasks. The study included the design of the suit, integration of FIAMs, and validation through human testing. The FIAMs, compliant with the human body and capable of generating sufficient force, were characterized for both linear and bending actuations. The results demonstrated minimal errors, highlighting the potential for practical applications with feedback control. Additionally, the lightweight anchoring design ensured comfort and minimal interference during use.

The experimental results revealed variations in the suit's impact on muscle activation and metabolic cost. Some participants showed reductions in normalized EMG ($iEMG_N$) and energy expenditure (*EEm*), while others exhibited negligible or inconsistent changes. Especially in <Off-On> case, participants experienced reductions in *EEm* during both the lifting and lowering phases, while participant 2 showed increased $iEMG_N$ and *EEm*. This highlights the importance of tailoring the suit design and actuator control strategies to achieve consistent benefits across users.

A comparison between the <None-On> and <Off-On> cases revealed that reductions in metabolic costs were more frequently observed. This indicates that wearing the suit without actuation increased muscle activation and energy expenditure, likely due to interference with natural movements [35], [36]. In contrast, active assistance provided by the suit in the <Off-On> case partially assisted the lifting motion by reducing the activation levels of the target muscles.

The results confirmed the feasibility of the suit in reducing muscle activation and metabolic cost, although variations among participants and muscle groups shows areas for improvement. These inconsistencies suggest the need for further refinement of the anchoring mechanism of the suit to ensure proper fit and alignment for all participants. Poor anchoring or misalignment may have contributed to increased effort or discomfort, as observed in certain cases, and warrants careful consideration in future examinations. Additionally, conducting more human trials under controlled clinical settings is necessary to refine the experimental methodology and validate the findings across diverse users and conditions.

Expanding the participant pool will be essential to draw robust statistical conclusions and establish reliable trends. However, before scaling the study, it is crucial to conduct iterative testing to optimize the suit design, particularly the anchoring mechanism, and evaluate the performance across repeated trials. A detailed analysis of the interaction between the suit and the human body will help address variability and ensure consistent benefits for a broader population.

Future work will include optimizing actuator control strategies to improve dynamic responsiveness and adaptability. Furthermore, expanding task-based evaluations, such as testing the maximum weight-lifting capacity or the assessing long-term usability, will help validate the functional benefits of the suit. These improvements will enhance the system's applicability in real-world scenarios, including industrial lifting, rehabilitation, and mobility support, while providing a foundation for more extensive clinical trials.

VI. CONCLUSION

The development of our assistive suit, equipped with artificial muscles, represents the progress in wearable technologies for

assisting labor-intensive tasks like lifting. While the participant sample size was limited, the result provides valuable insights into validating soft wearable technologies. The future research will focus on optimizing the anchoring suit for diverse users and tasks, expanding the participant pool, and refining actuator placement to enhance adaptability. This foundation paves the way for broader applications in industrial, rehabilitation, and mobility assistance settings, reducing metabolic cost and improving performance.

REFERENCES

[1] G. Agarwal, N. Besuchet, B. Audergon, and J. Paik, "Stretchable materials for robust soft actuators towards assistive wearable devices," *Sci. Rep.*, vol. 6, no. 1, pp. 1–8, 2016.

[2] Y.-L. Park et al., "Design and control of a bio-inspired soft wearable robotic device for ankle–foot rehabilitation," *Bioinspir. Biomim.*, vol. 9, no. 1, 2014, Art. no. 0 16007.

[3] J. Kwon, J.-H. Park, S. Ku, Y. Jeong, N.-J. Paik, and Y.-L. Park, "A soft wearable robotic ankle-foot-orthosis for post-stroke patients," *IEEE Robot. Autom. Lett.*, vol. 4, no. 3, pp. 2547–2552, Jul. 2019.

[4] J. I. Kim, J. Choi, J. Kim, J. Song, J. Park, and Y.-L. Park, "Bilateral back extensor exosuit for multidimensional assistance and prevention of spinal injuries," *Sci. Robot.*, vol. 9, no. 92, 2024, Art. no. eadk 6717.

[5] Y. Yang, Y. Wu, C. Li, X. Yang, and W. Chen, "Flexible actuators for soft robotics," *Adv. Intell. Syst.*, vol. 2, no. 1, 2020, Art. no. 1900077.

[6] C. Thalman and P. Artemiadis, "A review of soft wearable robots that provide active assistance: Trends, common actuation methods, fabrication, and applications," *Wearable Technol.*, vol. 1, 2020, Art. no. e3.

[7] J. Wirekoh, N. Parody, C. N. Riviere, and Y.-L. Park, "Design of fiber-reinforced soft bending pneumatic artificial muscles for wearable tremor suppression devices," *Smart Mater. Struct.*, vol. 30, no. 1, 2020, Art. no. 0 15013.

[8] S.-H. Park, J. Yi, D. Kim, Y. Lee, H. S. Koo, and Y.-L. Park, "A lightweight, soft wearable sleeve for rehabilitation of forearm pronation and supination," in *2nd IEEE Int. Conf. Soft Robot. (RoboSoft)*, IEEE, 2019, pp. 636–641.

[9] G. K. Klute, J. M. Czerniecki, and B. Hannaford, "Artificial muscles: Actuators for biorobotic systems," *Int. J. Robot. Res.*, vol. 21, no. 4, pp. 295–309, 2002.

[10] M. Li, A. Pal, A. Aghakhani, A. Pena-Francesch, and M. Sitti, "Soft actuators for real-world applications," *Nat. Rev. Mater.*, vol. 7, no. 3, pp. 235–249, 2022.

[11] J. Wirekoh, L. Valle, N. Pol, and Y.-L. Park, "Sensorized, flat, pneumatic artificial muscle embedded with biomimetic microfluidic sensors for proprioceptive feedback," *Soft Robot.*, vol. 6, no. 6, pp. 768–777, 2019.

[12] M. Ding, J. Ueda, and T. Ogasawara, "Pinpointed muscle force control using a power-assisting device: System configuration and experiment," in *Proc. IEEE RAS & EMBS Int. Conf. Biomed. Robot. Biomechatron.*, 2008, pp. 181–186.

[13] M. Pan et al., "Soft actuators and robotic devices for rehabilitation and assistance," *Adv. Intell. Syst.*, vol. 4, no. 4, 2022, Art. no. 2100140.

[14] J. Walker et al., "Soft robotics: A review of recent developments of pneumatic soft actuators," *Actuators*, vol. 9, no. 1, 2020, Art. no. 3.

[15] J. Wirekoh and Y.-L. Park, "Design of flat pneumatic artificial muscles," *Smart Mater. Struc.*, vol. 26, no. 3, 2017, Art. no. 0 35009.

[16] M. A. Robertson, H. Sadeghi, J. M. Florez, and J. Paik, "Soft pneumatic actuator fascicles for high force and reliability," *Soft Robot.*, vol. 4, no. 1, pp. 23–32, 2017.

[17] P. H. Nguyen and W. Zhang, "Design and computational modeling of fabric soft pneumatic actuators for wearable assistive devices," *Sci. Rep.*, vol. 10, no. 1, 2020, Art. no. 9638.

[18] R. S. Diteesawat, T. Helps, M. Taghavi, and J. Rossiter, "Electro-pneumatic pumps for soft robotics," *Sci. Robot.*, vol. 6, no. 51, 2021, Art. no. eabc3721.

[19] J. Kwon, S. J. Yoon, and Y.-L. Park, "Flat inflatable artificial muscles with large stroke and adjustable force– length relations," *IEEE Trans. Robot.*, vol. 36, no. 3, pp. 743–756, Jun. 2020.

[20] R. Niiyama, X. Sun, C. Sung, B. An, D. Rus, and S. Kim, "Pouch motors: Printable soft actuators integrated with computational design," *Soft Robot.*, vol. 2, no. 2, pp. 59–70, 2015.

[21] Y. Wang, Z. Ma, S. Zuo, and J. Liu, "A novel wearable pouch-type pneumatic artificial muscle with contraction and force sensing," *Sens. Actuators, A*, 2023, Art. no. 114506.

[22] N. Oh, Y. J. Park, S. Lee, H. Lee, and H. Rodrigue, "Design of paired pouch motors for robotic applications," *Adv. Mater. Technol.*, vol. 4, no. 1, 2019, Art. no. 1800414.

[23] Y. Kim, J. Kim, D. Lee, J. Piao, J. Bae, and S. H. Koo, "Development of clothing-type platforms considering pressure and user satisfaction: Focusing on industrial workers who tend to lift loads," *Text. Res. J.*, vol. 93, no. 9-10, pp. 2226–2241, 2023.

[24] M. Feng, D. Yang, L. Ren, G. Wei, and G. Gu, "X-crossing pneumatic artificial muscles," *Sci. Adv.*, vol. 9, no. 38, 2023, Art. no. eadi7133.

[25] C.-P. Chou and B. Hannaford, "Measurement and modeling of mckibben pneumatic artificial muscles," *IEEE Trans. Robot. Autom.*, vol. 12, no. 1, pp. 90–102, Jan. 1996.

[26] D. M. Rouffet and C. A. Hautier, "EMG normalization to study muscle activation in cycling," *J. Electromyogr. Kinesiol.*, vol. 18, no. 5, pp. 866–878, 2008.

[27] B. T. Kelly, L. W. Cooper, D. T. Kirkendall, and K. P. Speer, "Technical considerations for electromyographic research on the shoulder," *Clin. Orthop. Relat. Res. (1976-2007)*, vol. 335, pp. 140–151, 1997.

[28] J. Kim et al., "Reducing the energy cost of walking with low assistance levels through optimized hip flexion assistance from a soft exosuit," *Sci. Rep.*, vol. 12, no. 1, 2022, Art. no. 11004.

[29] L. Chen, C. Chen, Z. Wang, X. Ye, Y. Liu, and X. Wu, "A novel lightweight wearable soft exosuit for reducing the metabolic rate and muscle fatigue," *Biosensors*, vol. 11, no. 7, 2021, Art. no. 215.

[30] F. Peronnet et al., "Table of nonprotein respiratory quotient: An update," *Can. J. Sport Sci.*, vol. 16, no. 1, pp. 23–29, 1991.

[31] I. Perez-Suarez et al., "Accuracy and precision of the COSMED K5 portable analyser," *Front. Physiol.*, vol. 9, 2018, Art. no. 1764.

[32] R. A. Robergs, D. Dwyer, and T. Astorino, "Recommendations for improved data processing from expired gas analysis indirect calorimetry," *Sports Med.*, vol. 40, pp. 95–111, 2010.

[33] W. S. Marras et al., "Biomechanical risk factors for occupationally related low back disorders," *Ergonomics*, vol. 38, no. 2, pp. 377–410, 1995.

[34] I. Poitras, M. Bielmann, A. Campeau-Lecours, C. Mercier, L. J. Bouyer, and J.-S. Roy, "Validity of wearable sensors at the shoulder joint: Combining wireless electromyography sensors and inertial measurement units to perform physical workplace assessments," *Sensors*, vol. 19, no. 8, 2019, Art. no. 1885.

[35] R. C. Browning, J. R. Modica, R. Kram, and A. Goswami, "The effects of adding mass to the legs on the energetics and biomechanics of walking," *Med. Sci. Sports Exercise*, vol. 39, no. 3, pp. 515–525, 2007.

[36] A. Rodríguez-Fernández, J. Lobo-Prat, and J. M. Font-Llagunes, "Systematic review on wearable lower-limb exoskeletons for gait training in neuromuscular impairments," *J. NeuroEng. Rehabil.*, vol. 18, no. 1, p. 22, 2021.